Development 140, 1262-1271 (2013) doi:10.1242/dev.085316

Cofilin and Vangl2 cooperate in the initiation of planar cell polarity in the mouse embryo

James P. Mahaffey[1,2], Joaquim Grego-Bessa[1], Karel F. Liem, Jr[1,*] and Kathryn V. Anderson[1,‡]

SUMMARY

The planar cell polarity (PCP; non-canonical Wnt) pathway is required to orient the cells within the plane of an epithelium. Here, we show that cofilin 1 (Cfl1), an actin-severing protein, and Vangl2, a core PCP protein, cooperate to control PCP in the early mouse embryo. Two aspects of planar polarity can be analyzed quantitatively at cellular resolution in the mouse embryo: convergent extension of the axial midline; and posterior positioning of cilia on cells of the node. Analysis of the spatial distribution of brachyury$^+$ midline cells shows that the *Cfl1* mutant midline is normal, whereas *Vangl2* mutants have a slightly wider midline. By contrast, midline convergent extension fails completely in *Vangl2 Cfl1* double mutants. Planar polarity is required for the posterior positioning of cilia on cells in the mouse node, which is essential for the initiation of left-right asymmetry. Node cilia are correctly positioned in *Cfl1* and *Vangl2* single mutants, but cilia remain in the center of the cell in *Vangl2 Cfl1* double mutants, leading to randomization of left-right asymmetry. In both the midline and node, the defect in planar polarity in the double mutants arises because PCP protein complexes fail to traffic to the apical cell membrane, although other aspects of apical-basal polarity are unaffected. Genetic and pharmacological experiments demonstrate that F-actin remodeling is essential for the initiation, but not maintenance, of PCP. We propose that Vangl2 and cofilin cooperate to target Rab11$^+$ vesicles containing PCP proteins to the apical membrane during the initiation of planar cell polarity.

KEY WORDS: Rab11, Axial midline, Cilia, Convergent extension, Left-right patterning, Planar polarity, Mouse, Myosin light chain

INTRODUCTION

The non-canonical Wnt/PCP pathway is an evolutionarily conserved process that polarizes cells in the plane of an epithelial sheet in the dimension orthogonal to the apical-basal axis of the cells. The output of this signaling pathway can be seen in the uniform orientation of cellular processes, such as the wing hairs in *Drosophila*, or in multicellular structures like the fur on mice (Vinson and Adler, 1987; Devenport and Fuchs, 2008). Genetic screens in *Drosophila* identified an evolutionarily conserved group of core PCP proteins – Flamingo, van Gogh/Strabismus, Frizzled, Dishevelled (Dvl), Prickle and Diego – that confer planar polarity and control cell orientation in the developing eye ommatidia, larval cuticle and wing epithelium. The core PCP proteins are present in two distinct protein complexes, the Van Gogh and Frizzled complexes, that are localized to the apical membrane on opposite sides of individual cells (Axelrod, 2001; Tree et al., 2002; Bastock et al., 2003). In the *Drosophila* wing, Frizzled/Dvl complexes activate downstream effectors of the PCP pathway, including Rac1, RhoA, ROCK and DAAM, on the distal side of the cell, ultimately regulating formation of the actin-based wing hair (Eaton et al., 1996; Strutt et al., 1997; Winter et al., 2001; Matusek et al., 2006).

At the early stages of *Drosophila* pupal wing development, the core PCP proteins are present in puncta within the cytoplasm; later, they become uniformly distributed around the apical cell membrane. Prior to wing hair formation, the van Gogh and Frizzled complexes are segregated to proximal and distal faces of the cell, respectively, and are excluded from the anterior and posterior faces of the cell (Usui et al., 1999; Strutt, 2001). Thus, planar polarity in *Drosophila* is achieved in two steps: first, the core PCP proteins move to the apical cell membrane at the level of the adherens junctions; second, they are segregated within the apical membrane into two complexes (Strutt and Strutt, 2008; Wu and Mlodzik, 2008).

Experiments in *Drosophila* have implicated Cofilin, a regulator of the actin cytoskeleton, in the initiation of planar polarity. Cofilin severs F-actin filaments, an essential step in remodeling the actin cytoskeleton. *Drosophila* homozygous for a temperature-sensitive *Cofilin* allele show PCP phenotypes in the eye and wing, owing to decreased association of Frizzled and Flamingo with the plasma membrane (Blair et al., 2006). These results suggested that actin dynamics have a role in the establishment of planar polarity, in addition to a role downstream of PCP to build wing hairs.

Mutations in mouse core PCP genes disrupt embryonic morphogenesis, affecting the shape of the somites, notochord and cochlea. A hallmark of mouse PCP mutants is craniorachischisis, a failure to close the neural tube in all regions caudal to the midbrain (Copp et al., 2003). Craniorachischisis in these mutants has been attributed to defects in convergent extension (CE), a morphogenetic process that leads to mediolateral narrowing and anterior-posterior elongation through mediolateral intercalation (Keller, 2002). Other aspects of CE, such as narrowing of the somites, are only mildly affected in mouse single PCP mutants, such as *Vangl2*, in contrast to the stronger defects in somite shape observed when single PCP genes are knocked down in *Xenopus*, in zebrafish (Greene et al., 1998; Park and Moon, 2002; Wallingford and Harland, 2002; Darken et al., 2002) or in mouse *Vangl1 Vangl2* double mutants (Song et al., 2010).

Two aspects of PCP can be characterized quantitatively at cellular resolution in the early mouse embryo: elongation of the axial

[1]Developmental Biology Program, Sloan-Kettering Institute, 1275 York Avenue, New York, NY 10065, USA. [2]Louis V. Gerstner Jr. Graduate School of Biomedical Sciences, Memorial Sloan-Kettering Cancer Center, 1275 York Avenue, New York, NY 10065, USA.

*Present address: Department of Pediatrics, Yale School of Medicine, New Haven, CT 06520, USA
‡Author for correspondence (k-anderson@sloankettering.edu)

Accepted 3 January 2013

mesendoderm (the notochordal plate) and positioning of nodal cilia. The midline is formed from cells that migrate rostrally from the node and eventually lie under the neural plate, inducing the floor plate of the neural tube. Tissue-level analysis has shown that the notochordal plate and floor plate are wider in PCP mutants (Greene et al., 1998; Wang et al., 2006; Ybot-Gonzalez et al., 2007); here, we use high resolution imaging to define the cellular basis of PCP-dependent narrowing of the midline. The initiation of left-right asymmetry also depends on planar polarity. Leftward fluid flow across the node, which is necessary and sufficient to establish left side-specific gene expression, depends on posterior positioning of cilia on each cell of the node (Nonaka et al., 1998; Nonaka et al., 2002; Nonaka et al., 2005). The PCP pathway is required for this posterior location, as the basal bodies of cilia remain at the middle of the cells of the node in *Vangl1 Vangl2* double mutants and the *Dvl1/Dvl2/Dvl3* compound mutants (Hashimoto et al., 2010; Song et al., 2010), although basal body position and left-right asymmetry is normal in each of the single mutants.

The stronger phenotypes of the *Vangl1 Vangl2* double mutants and the *Dvl1/Dvl2/Dvl3* compound mutants compared with single PCP mutants provide a tool to identify other proteins required for planar cell polarity. To test whether cofilin plays a role in mammalian PCP, we analyzed the phenotypes of double mutants that lacked normal activity of both Vangl2 and cofilin 1. These double mutant embryos had PCP phenotypes as strong as those seen in *Vangl1 Vangl2* double mutants, including short and wide somites, failure of convergent extension of the midline, and randomization of left/right asymmetry caused by the failure to properly polarize nodal cilia. We show that cofilin acts in concert with Vangl2 during the initiation of PCP to control the initial asymmetric localization of the core PCP protein Celsr1 to the apical membrane. Thus, dynamic rearrangements of the actin cytoskeleton are required for the establishment of PCP signaling in the mouse. We propose a model for the initiation of PCP in the mouse in which remodeling of the actin cytoskeleton has an essential role in the trafficking of $Rab11^+$ PCP^+ vesicles to their appropriate planar polarized locations in the apical plasma membrane.

MATERIALS AND METHODS

Mouse strains

The *C5* mutation was isolated in a C57BL6/J chromosome in a genome-wide screen for N-ethyl N-nitrosourea (ENU)-induced recessive mutations (García-García et al., 2005). *C5* was mapped using simple sequence length polymorphism (SSLP) markers from the MIT database and new polymorphic markers to the proximal region of chromosome 19, a region that included *Cfl1*. The *C5* allele had a single T to A transversion in the *Cfl1*-coding sequence, leading to an F101I missense substitution. $Cfl1^{C5}/Cfl1^{tm1Wit}$ embryos had a similar phenotype to the $Cfl1^{C5}$ and $Cfl1^{tm1Wit}$ homozygous phenotypes, indicating that this single amino acid substitution caused a strong loss of cofilin 1 function. The $Cfl1^{tm1Wit}$ null allele was a gift from Walter Witke (Rheinische Friedrich-Wilhelms University, Bonn, Germany). The $Cfl1^{C5}$ mutation created a *Bcl*I restriction site used for genotyping. The $Vangl2^{Lp}$ and $Dstn^{corn1}$ mice were from The Jackson Laboratory. $IFT88^{tm1.1Bky}$ ($IFT88^{-}$) mice were provided by Bradley Yoder (The University of Alabama at Birmingham, AL, USA).

Phenotypic analysis and embryo culture

Embryos were dissected in ice-cold PBS/4% BSA and processed for imaging following previously established protocols (Lee et al., 2010). Brachyury (T) antibody, a gift from Frank Conlon (UNC-Chapel Hill, NC, USA), was used at 1:3200. Celsr1 antibody (Devenport and Fuchs, 2008), a gift from Elaine Fuchs (The Rockefeller University, New York, USA), was used at 1:800. Vangl2 antibody (Montcouquiol et al., 2006), a gift from Mireille Montcouquiol (University of Bordeaux, France), was used at 1:800. Cofilin antibody (Sigma) was diluted 1:1000, E-cadherin (Sigma) was diluted 1:1000, EEA1 (Abcam) was diluted 1:800, fibronectin (Sigma) was diluted 1:2500, GM-130 (BD Biosciences) was diluted 1:800, Par3 (Millipore) was diluted 1:1000, pericentrin (Covance) was diluted 1:800, phospho-myosin light chain 2 (Cell Signaling) was diluted 1:200, Rab5 (Cell Signaling) was diluted 1:400, Rab8 (BD Biosciences) was diluted 1:400, Rab11 (Cell Signaling) was diluted 1:400, α-tubulin (Sigma) was diluted 1:5000 and ZO-2 (BD Biosciences) was diluted 1:1000. After mounting, slides were imaged with a LSM510 confocal microscope (Zeiss) or a DeltaVision microscope (Applied Precision). Images taken with the DeltaVision were deconvolved after imaging. Databases were analyzed using the Volocity software suite (Improvision). Unless otherwise noted, all confocal images are single optical slices. The immunofluorescence data presented in the figures are representative images of at least three stained embryos per genotype/drug treatment.

In situ hybridization staining was performed using standard protocols. Samples for SEM were dissected in ice-cold PBS and fixed overnight in 2.5% glutaraldehyde, then processed and observed according to standard procedures (Sulik et al., 1994) using a Zeiss Supra 25 Field Emission Scanning Electron Microscope.

Embryos for culture were dissected in 37°C DMEM/F12 containing 20% FBS. After dissection, embryos were transferred to a glass-bottomed culture dish. Static embryo cultures were performed in media containing 50% rat serum/50% DMEM/F12 and incubated at 37°C with 5% CO_2 for 14-18 hours. A stock of jasplakinolide (Sigma) in DMSO was diluted in the culture medium to 10 nM (0.01% DMSO). A stock of IWP-2 (Sigma) in DMSO was diluted in the culture medium to 5 μM (0.1% DMSO); control embryos were cultured in 0.1% DMSO.

Image analysis and statistics

To analyze the distribution of T-positive notochordal plate cells, the Cell-Counter plugin for ImageJ software (NIH) was used to count every T^+ nucleus in a row of the notochord. The number of rows counted was used to find the length of the tissue. Measurements of the stained tissue were made using the line draw feature of Volocity; this was also used to determine the length to width ratio (LWR) of *Meox1*-stained somites. The midline width measurements are an average of ten equally spaced lines, ranging from the beginning to the end of the notochordal plate.

To determine the relative position of the basal body, we outlined individual cells from the central node region using ImageJ and measured the length of the *y*-axis (parallel to the anterior-posterior axis of the embryo). We then determined the position of the basal body by finding the center of mass of the pericentrin signal by isolating a coordinate point within the cell.

To quantify the degree of planar polarization of Celsr1, we imported images containing Celsr1 and phalloidin staining into hyperstacks in ImageJ. We then traced cell borders with individual lines along the phalloidin channel and quantified the average pixel intensity for both phalloidin and Celsr1 staining, then normalized the Celsr1 intensity to the phalloidin signal. We organized the data according to the angle of the line that was drawn. For all images and quantification, the anterior of the embryo is toward the top. We measured the intensities from 40 node cells per embryo, which totaled ~150 cell borders (owing to shared borders); two embryos per genotype were quantified. All statistical analysis was performed using PRISM software; all values are shown as averages±s.d., and data were analyzed with one-way ANOVA followed by the Newman-Keuls post-test.

RESULTS

Removal of *Cfl1* strongly enhances the phenotype of *Vangl2* mouse mutants

We isolated a strong missense allele of cofilin 1 (*Cfl1*, also called non-muscle cofilin, one of three mouse cofilin genes) in a screen for recessive N-ethyl N-nitrosourea (ENU)-induced recessive mutations that caused morphological defects in midgestation mouse embryos. At E9.5, there was a significant decrease in the amount of Cfl1 protein in homozygotes (supplementary material Fig. S1F). The mutants had an open cranial neural tube, a closed neural tube in the trunk and defects in outflow tract development that caused pericardial edema (Fig. 1B), similar to the phenotype of a null allele of *Cfl1* (supplementary material Fig. S1A) (Gurniak et al., 2005).

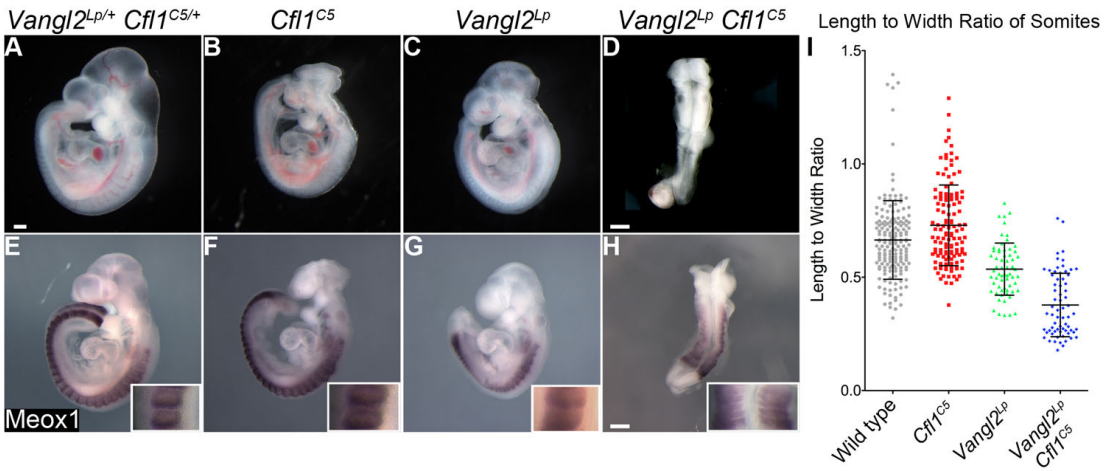

Fig. 1. Genetic interaction between *Vangl2^{Lp}* and *Cfl1^{C5}* at E9.5. (**A**) A *Vangl2$^{Lp/+}$ Cfl$^{C5/+}$* embryo, which is indistinguishable from wild type. (**B**) *Cfl1^{C5}* homozygote. Homozygous mutants are exencephalic and die ~E11.0. (**C**) *Vangl2^{Lp}* homozygote. Homozygous mutant embryos have an open neural tube caudal to the midbrain-hindbrain junction. (**D**) *Vangl2^{Lp} Cfl^{C5}* double mutant. These embryos have a completely open neural tube, a short body axis and abnormal somites. (**E-H**) *Meox1 in situ* hybridization (purple) highlights the somites; there are wide somites in the double mutant (H). Insets show a 4× higher magnification of somites. (**I**) The length to width ratio (LWR) of somites. Somites in *Vangl2^{Lp}* mutants are significantly shorter and wider than wild-type or *Cfl^{C5}* embryos (P<0.001). Somites in *Vangl2^{Lp} Cfl^{C5}* double mutants have significantly reduced LWR compared with wild type or either single mutant (P<0.001); *Vangl2^{Lp} Cfl^{C5}* double mutants had 20-22 somite pairs and other genotypes had 22-28 at the stage analyzed. Scale bars: 250 μm. Data are mean±s.d.

Despite the role of cofilin in the PCP pathway in *Drosophila* (Blair et al., 2006), *Cfl1^{C5}* mutants did not show hallmark PCP phenotypes. However, removal of another PCP protein can enhance the relatively weak phenotypes of *Vangl2* mutations (Song et al., 2010); therefore, to test whether cofilin has a role in the mouse PCP pathway, we generated *Vangl2^{Lp} Cfl1^{C5}* double mutants. The E9.5 *Vangl2^{Lp}* neural tube was open from the hindbrain to the tail (craniorachischisis) (Fig. 1C), whereas the *Cfl1^{C5}* neural tube was closed caudal to the hindbrain. The E9.5 *Vangl2^{Lp} Cfl1^{C5}* double mutant embryos had a stronger phenotype than either single mutant: they were shorter, had an open neural tube along the entire axis of the embryo, failed to undergo embryonic turning and arrested at ~E9.5 (Fig. 1D); a similar phenotype was seen in *Vangl2^{Lp} Cfl1^{null}* double mutants (supplementary material Fig. S1B).

The PCP pathway is required for the convergent extension (CE) movements that extend the anterior-posterior body axis of the vertebrate embryo. *Xenopus* morphants and zebrafish mutants that lack Vangl2 or other core pathway components have short and wide somites, suggesting that convergent extension is required in the paraxial mesoderm for normal somite morphology (Park and Moon, 2002; Veeman et al., 2003). Somite shape in mouse *Vangl2* embryos is relatively normal, but *Vangl1 Vangl2* double mutants have somites that are short along the anterior-posterior axis and wide mediolaterally (Song et al., 2010). *Vangl2^{Lp} Cfl1^{C5}* double mutant embryos also appeared to have wide somites. We measured the length-to-width ratio (LWR) of the somites of *Meox1*-stained embryos (Fig. 1E-H), where length is the distance along the anterior-posterior axis, and width is the mediolateral distance. *Cfl1^{C5}* somites were similar in shape to those in wild-type littermates, with a LWR of 0.66±0.17 in wild type and 0.73±0.18 in the mutant. *Vangl2^{Lp}* somites were shorter and wider, with a LWR of 0.54±0.11 (P<0.001). The somites of *Vangl2^{Lp} Cfl1^{C5}* double mutants were significantly wider than *Vangl2^{Lp}* single mutants, with a LWR of 0.38±0.14 (P<0.001) (Fig. 1I), similar to what was reported in *Vangl1 Vangl2* double mutants (Song et al., 2010). These data show that cofilin 1 works together with Vangl2 to control the shape of somites in the mouse embryo.

Convergent extension of the midline fails in *Vangl2 Cfl1* double mutant embryos

Previous observations based on histological analysis and *in situ* hybridization with midline markers suggested that the axial midline of *Vangl2^{Lp}* mutants is shorter and wider than that of wild-type embryos (Greene et al., 1998; Ybot-Gonzalez et al., 2007). To determine whether the morphogenetic defects in the *Vangl2^{Lp} Cfl1^{C5}* double mutants were due to true defects in CE, we analyzed the cellular organization of the axial midline. The notochordal plate of the one- to four-somite stage embryo is a single layer epithelium that lies on the surface of the embryo, allowing imaging at a cellular resolution. At this stage, cells of the midline are quiescent (Bellomo et al., 1996), so cell division does not complicate the analysis of midline morphogenesis. One- to four-somite stage *Vangl2^{Lp} Cfl1^{C5}* embryos were similar in size and global morphology to wild-type embryos; therefore, changes in the organization of the midline were likely to be a primary defect. To visualize individual cells in the midline, we stained E8.0 embryos with an antibody against brachyury (T), which specifically labels the nuclei of cells in the node and midline (Fig. 2A-D′).

Embryos of all four genotypes (wild type, *Vangl2^{Lp}*, *Cfl1^{C5}* and *Vangl2^{Lp} Cfl1^{C5}*) at the one- to four-somite stage had indistinguishable numbers of brachyury-positive cells in the midline (wild type, 200±14; *Vangl2^{Lp}*, 205±22; *Cfl1^{C5}*, 199±33; *Vangl2^{Lp} Cfl1^{C5}*, 195±24). The notochordal plate of wild-type embryos was 3.7±0.3 cells in width and 54.7±6.3 cells long (AP axis) (Fig. 2A). The *Cfl1^{C5}* single mutant midline was not significantly different from wild type (3.7±0.4 cells wide and 53.3±9.5 cells long) (Fig. 2B). The midline of *Vangl2^{Lp}* single mutants was significantly wider and shorter (4.5±0.5 cells wide and 45.8±7.1 cells long) (Fig. 2C), confirming earlier histological observations (Greene et al., 1998; Wang et al., 2006; Ybot-Gonzalez et al., 2007).

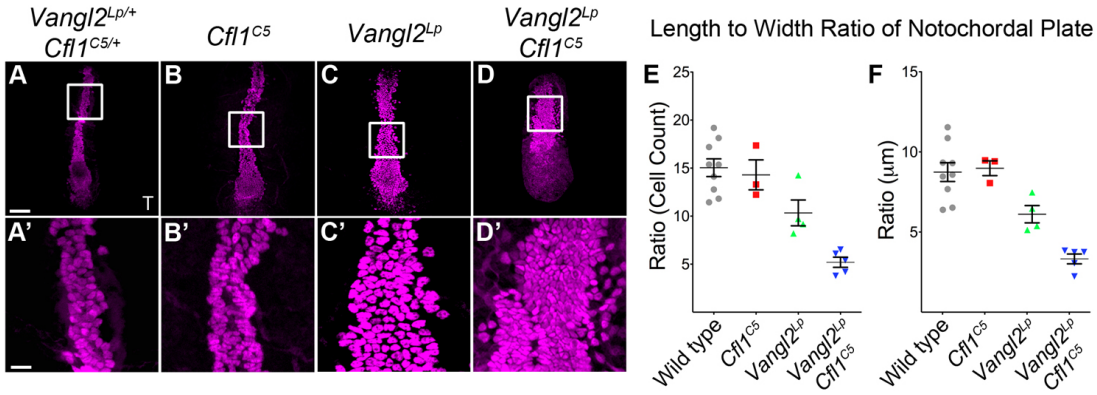

Fig. 2. *Cfl1*^{C5} enhances the convergent extension defect in the *Vangl2*^{Lp} notochord. (**A-D**) Projections of flat-mounted E8.0 embryos stained for brachyury (T) (magenta). (**A′-D′**) Higher magnifications (4×) of midline cells from boxed regions of A-D highlight the arrangement of cells in each genotype. Wild type (A) and *Cfl1*^{C5} (B) have a similar arrangement of T^{+} cells in the midline, whereas the *Vangl2*^{Lp} midline (C) is wider and shorter. The *Vangl2*^{Lp} *Cfl1*^{C5} mutant midline (D) is wider and shorter than *Vangl2*^{Lp}. (**E**,**F**) The LWR of the notochordal plate measured by the distribution of cells (E) or in µm (F). Scale bars: 100 µm in A-D; 25 µm in A′-D′. Data are mean±s.d.

Vangl2^{Lp} *Cfl1*^{C5} double mutant embryos showed a stronger midline defect than *Vangl2*^{Lp} single mutants. The midline of double mutants was shorter and wider (6.21±0.8 cells wide and 31.6±4.3 cells long) than *Vangl2*^{Lp} or *Cfl1*^{C5} single mutants (Fig. 2D). When calculated in terms of LWR, the *Vangl2*^{Lp} *Cfl1*^{C5} double mutant was threefold shorter and wider than wild type, and twofold shorter and wider than *Vangl2*^{Lp} (LWR: in wild-type and *Cfl1*^{C5} embryos, 14-15; *Vangl2*^{Lp}, 10.3; *Vangl2*^{Lp} *Cfl1*^{C5} double mutant, 5.2) (Fig. 2E). This phenotype was not due to changes in cell shape, as we measured similar decreases in the LWR in *Vangl2*^{Lp} mutants and *Vangl2*^{Lp} *Cfl1*^{C5} double mutants (compared with wild type or *Cfl1*^{C5}) when the dimensions of the notochordal plate were measured in µm rather than cell number (Fig. 2F). Thus, convergent extension of the axial midline depends on both Vangl2 and Cfl1.

Cofilin 1 and PCP signaling cooperate to orient nodal cilia during the establishment of left/right asymmetry

Of six *Vangl2*^{Lp} *Cfl1*^{C5} double mutants examined at E9.5, one embryo had a linear heart tube and two showed left-right reversal of heart looping, a phenotype not seen in either single mutant (Fig. 3A-C). Like wild-type embryos, *Cfl1*^{C5} and *Vangl2*^{Lp} single mutants expressed the left-sided marker *Nodal* exclusively on the left side of the embryo in the lateral plate mesoderm at E8.5 and showed stronger expression of *Nodal* on the left side of the node at E8.0. By contrast, four out of seven double mutant embryos examined showed either bilateral expression of the *Nodal* gene at E8.5 (Fig. 3D-F′) or stronger staining on the right side of the node at E8.0 (Fig. 3G-I), indicating that left-right is randomized in these double mutants.

The first event in the establishment of left-right asymmetry in the mouse embryo is the planar polarization of cells in the mouse node. Between the early and late headfold stages, the cilium on each node cell moves from the center to the posterior side of the cell such that cilia tilt towards the posterior; because of the posterior tilt of the cilia, their beating creates a fluid flow toward the left side of the node (Nonaka et al., 2005; Hashimoto et al., 2010). Previous studies have shown that the cilia remain at the center of the cell in PCP compound mutants, which causes randomization of sidedness (Hashimoto et al., 2010; Song et al., 2010; Shinohara et al., 2012). In SEM images of wild-type, *Cfl1*^{C5} and *Vangl2*^{Lp} single mutant embryos, node cilia pointed posteriorly and appeared to emanate from the posterior face of the cell (Fig. 4A,C,E). SEM images of *Vangl2*^{Lp} *Cfl1*^{C5} double mutant nodes at the two-somite stage showed that node cilia of normal length were present, but they did not point uniformly to the posterior and their position on the cell appeared more variable than in wild type or the single mutants (Fig. 4G; supplementary material Fig. S2).

Staining of whole-mount embryos at the two- to four-somite stages with pericentrin, a protein localized at the ciliary basal body, showed that the majority of the basal bodies in wild-type, *Vangl2*^{Lp} and *Cfl1*^{C5} node cells were polarized towards the posterior side of the cell (Fig. 4B,D,F). By contrast, there were many cells in *Vangl2*^{Lp} *Cfl1*^{C5} double mutants where the pericentrin staining was localized towards the anterior side of the cell (Fig. 4H). We used the immunofluorescence images to measure the relative position of the basal body along the *y*-axis (the posterior to the anterior face) of the cell. The position of the basal body was calculated by dividing the coordinate of the center of mass of the pericentrin staining by the length of the cell along the *y*-axis, such that a basal body residing on the posterior face of the cell would have a value of zero, and one on the anterior face of the cell would have a value of one. The basal body was polarized to the posterior side of node cells in wild type and in both single mutants [the position was 0.37±0.09 in wild type (n=536); 0.37±0.09 in *Cfl1*^{C5} (n=193) and 0.36±0.08 in *Vangl2*^{Lp} (n=187)]. By contrast, the basal bodies of *Vangl2*^{Lp} *Cfl1*^{C5} double mutants were located near the center of the cell [average basal body position=0.46±0.11(n=307)], significantly different from the other genotypes (P<0.001) (Fig. 4I). The variance of basal body position was also significantly increased in the double mutant (P<0.001). Thus, the basal bodies in the *Vangl2*^{Lp} *Cfl1*^{C5} double mutants failed to polarize to the posterior of the cell.

Cofilin 1 is important for the polarized localization of PCP proteins in the node

To define the mechanism that led to cilia mispositioning and convergent extension defects in *Vangl2*^{Lp} *Cfl1*^{C5} double mutants, we analyzed the subcellular localization of core PCP proteins. As in the *Drosophila* wing disc and mouse inner ear (Strutt, 2001; Montcouquiol et al., 2006), the core PCP proteins localize to opposing faces within the cells of the node (Hashimoto et al., 2010;

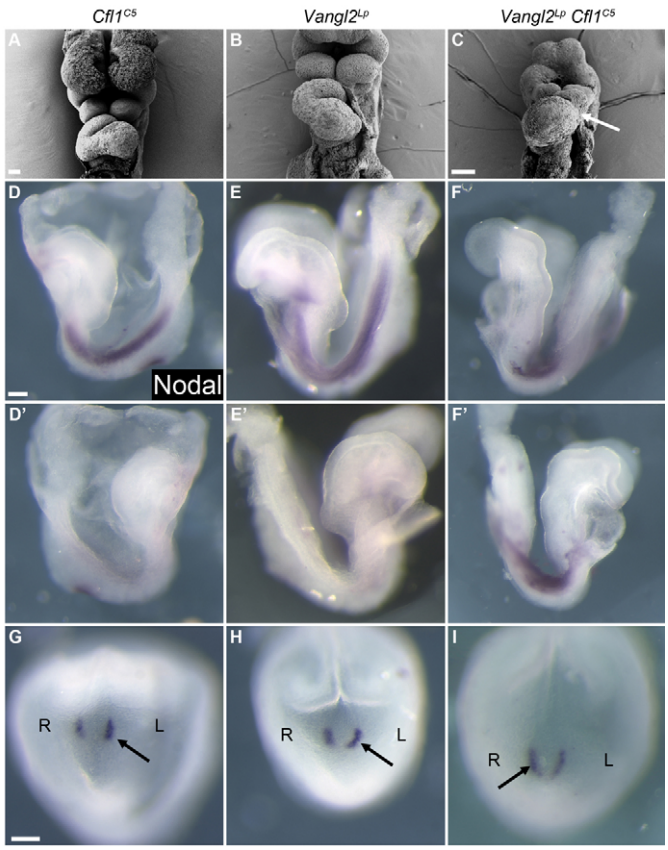

Fig. 3. Defects in left-right asymmetry in *Vangl2^{Lp} Cfl1^{C5}* double mutant embryos. (**A-C**) A fraction of *Vangl2^{Lp} Cfl1^{C5}* double mutants examined at E9.5 showed reversed heart looping (arrow), a phenotype not seen in either single mutant. (**D-I**) This phenotype is due to an early defect in left-right asymmetry, as some double mutants express *Nodal* (purple) bilaterally in the lateral plate mesoderm and show increased *Nodal* expression on the right side of the node. Arrows indicate the side of the node with stronger *Nodal* expression. Scale bars: 100 μm.

Song et al., 2010). As previously reported for Vangl1/2 and GFP-tagged Dvl1/2, we observed that Celsr1 (the Flamingo homologue) was highly enriched along the anterior/posterior borders of wild-type node cells and was excluded from the mediolateral faces of the cells. To quantitate the planar polarization of Celsr1, we measured the mean fluorescence intensity of the Celsr1 signal along all edges of cells within the ventral node. In wild-type embryos, there was a twofold enrichment of Celsr1 on the anterior/posterior faces of the cell compared with the mediolateral sides (Fig. 5A,B; supplementary material Fig. S3A). The same polarization of Celsr1 was seen in *Vangl2^{Lp}* and *Cfl1^{C5}* single mutants (Fig. 5C-F; supplementary material Fig. S3B,C). By contrast, Celsr1 was not enriched at any membrane of *Vangl2^{Lp} Cfl1^{C5}* double mutant node cells (Fig. 5G-H; supplementary material Fig. S3D) or *Vangl2^{Lp} Cfl1^{null}* double mutants (supplementary material Fig. S1D), indicating that cofilin 1 directly regulated PCP protein polarization.

The defect in Celsr1 localization in the double mutant embryos appeared to be specific to the PCP pathway, as we did not detect defects in other apically localized proteins, including Par3, E-cadherin and ZO2, or in the basal localization of fibronectin (supplementary material Fig. S4). SEM analysis also indicated that every cell in the node had a single cilium, and pericentrin staining showed that there were apically docked basal bodies in every cell (Fig. 4G-H), consistent with normal apical/basal polarity in the *Vangl2^{Lp} Cfl1^{C5}* double mutant node cells.

Several studies have suggested that there is a complex relationship between cilia and the PCP pathway, proposing a link between the polarization of cytoskeleton and ciliogenesis (Ross et al., 2005; Jones et al., 2008). To test whether cilia play a role in PCP signaling in the node, we generated E8.0 *Ift88*-null embryos and stained them for pericentrin, Celsr1 and Vangl2. We found no defect in the positioning of the basal body in the *Ift88$^{-/-}$* embryos compared with wild-type littermates (0.36±0.09 and 0.38±0.09, respectively). Celsr1 and Vangl2 proteins were apically enriched in the plasma membrane on the anterior/posterior faces of the cell in embryos lacking *Ift88*, as in wild-type littermates (supplementary material Fig. S5). We conclude that the primary cilium is dispensable for the establishment of planar cell polarity in the E8.0 node, ruling out the possibility that misplaced cilia in the *Vangl2^{Lp} Cfl1^{C5}* node are responsible for the mislocalization of Celsr1 and Vangl2 in these cells.

Loss of actin-severing activity is sufficient to disrupt planar polarity in the node

There are three cofilin genes in the mouse. *Cfl2* is expressed specifically in muscle. *Cfl1* and destrin [*Dstn*, or actin depolymerizing factor (ADF)] are broadly expressed throughout development (Gurniak et al., 2005). Animals homozygous for a deletion removing the *Dstn* locus, *Dstn^{corn1}*, are viable and fertile, but show a thickening of the cornea in adults (Smith et al., 1996). Cfl1 and Dstn may overlap in function, as destrin protein is upregulated in *Cfl1*-null mutants (Gurniak et al., 2005). To test whether actin-severing activity is required for PCP signaling in the presence of wild-type Vangl2, we analyzed PCP protein localization in *Cfl1^{C5}* embryos with reduced Dstn activity. We were unable to recover *Cfl1^{C5} Dstn^{corn1}* double mutants at post-implantation stages, suggesting that actin severing is essential for pre-implantation development. Although the majority of the *Cfl1^{C5} Dstn$^{corn1/+}$* embryos arrested prior to node formation, we recovered three embryos that developed nodes. In contrast to *Cfl1$^{C5/+}$ Dstn$^{corn1/+}$* littermates, both Celsr1 and Vangl2 localized to cytoplasmic puncta that were dispersed throughout the apical cytoplasm in the *Cfl1^{C5} Dstn$^{corn1/+}$* mutant nodes, providing evidence that the stabilization of actin filaments is sufficient to prevent membrane association of PCP proteins (Fig. 6A,B).

Dynamic rearrangements of the actin cytoskeleton are required for initiation, but not maintenance, of planar polarization of Vangl2 and Celsr1

In an independent test of the role of actin dynamics in mouse PCP, we stabilized actin filaments pharmacologically using jasplakinolide (Bubb et al., 1994). We cultured wild-type embryos in 10 nM jasplakinolide, a concentration that phenocopied the effects of a dominant-negative cofilin in the mouse yolk sac (Koike et al., 2009). At late-bud stage (E7.25), the node is not mature, and Vangl1 and Vang2 are not yet planar polarized in the membrane (Song et al., 2010). When wild-type E7.25 embryos were cultured for 15 hours in the absence of drug, Celsr1 became planar polarized in node cells during the period of culture (Fig. 6E,F; supplementary material Fig. S3E). By contrast, when wild-type embryos at the same stage were cultured in the presence of jasplakinolide, Celsr1 and Vangl2 did not become enriched in the apical membrane in either the node or the midline (Fig. 6D; Fig. 7B; supplementary material Fig. S6B),

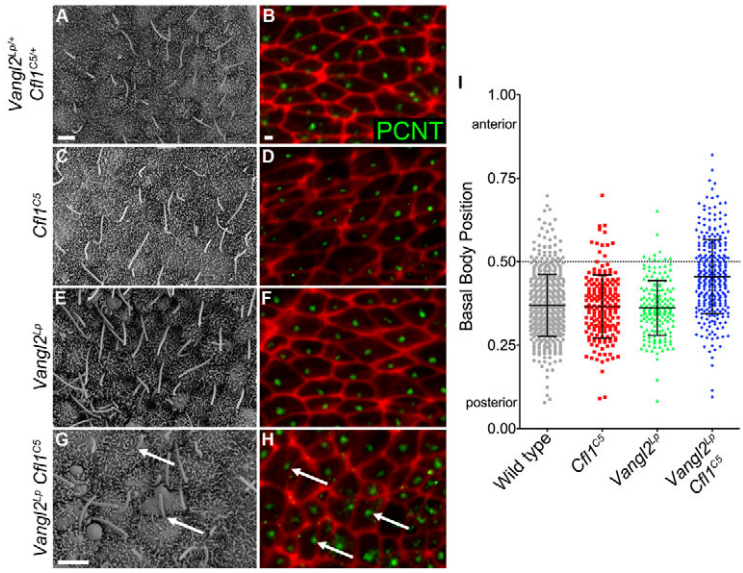

Fig. 4. Nodal cilia are not posteriorly positioned in *Vangl2^{Lp} Cfl1^{C5}* double mutants. (**A**,**C**,**E**) Scanning electron microscope images of the node show that cilia are polarized to the posterior of node cells in wild type, *Cfl1^{C5}* and *Vangl2^{Lp}* single mutants. (**B**,**D**,**F**) Basal bodies, visualized by the centrosomal protein pericentrin (green), show a similar posterior position in the cells of wild type, *Cfl1^{C5}* and *Vangl2^{Lp}* single mutants. F-actin at the cell borders is highlighted with phalloidin (red). (**G**) In *Vangl2^{Lp} Cfl1^{C5}* double mutants, many cilia point anteriorly (arrows). (**H**) Many basal bodies are mislocalized to the anterior half of the cell in *Vangl2^{Lp} Cfl1^{C5}* double mutants (arrows). Anterior is towards the top in all images. (**I**) The relative localization of basal bodies in individual central node cells was quantified from immunofluorescence images from at least three embryos per genotype. The graph shows that basal bodies in double mutants are not positioned on the posterior of cells; in addition, there is a greater variance in the placement of cilia compared with wild type or either single mutant. Data are mean±s.d. Scale bars: 2 µm.

whereas markers of apical-basal polarity were maintained (supplementary material Fig. S4M-O). As in *Vangl2^{Lp} Cfl1^{C5}* and *Cfl1^{C5} Dstn$^{corn1/+}$* mutants, Celsr1 and Vangl2 were present in cytoplasmic puncta in the apical domain of the cells. The puncta of Celsr1 and Vangl2 staining in these embryos appear to represent post-Golgi vesicles, as they were found apical to GM130, a marker of the cis-Golgi network (supplementary material Fig. S6B).

At a later stage, after formation of the node (~E7.75), culture in the presence of jasplakinolide did not affect the localization of Celsr1 in the node, which was planar polarized at the membrane in both treated embryos and controls (Fig. 6C). This stage-dependent effect is probably responsible for the variability of Celsr1 staining in jasplakinolide-treated embryos (compare Fig. 6D; Fig. 8B,D; supplementary material Fig. S7B,D). The findings indicate that cofilin is required for the initiation, but not the maintenance, of planar polarity in the mouse node.

To test whether the loss of Celsr1 in the apical membrane was a consequence of the loss of PCP pathway activity, we compared the localization of Celsr1 in *Vangl2^{Lp} Cfl1^{C5}* double mutants to its localization in the absence of Wnt ligand. To block ligand production, we cultured E7.25 wild-type embryos in the presence of 5 µM IWP2, a small molecule inhibitor of the glycosyl-transferase porcupine, which is required for secretion of Wnt ligands (Chen et al., 2009). After culture with IWP2, Celsr1 was recruited to the apical membrane of node cells but planar polarity was disrupted: unlike DMSO control cultures, Celsr1 was no longer restricted solely to the anterior/posterior faces of node cells. Within the same node, Celsr1 was enriched on the medial/lateral faces (60-89°) in some cells and anterior/posterior faces (0-30°) in other cells, demonstrating that Wnt ligand is not required for membrane localization or even restriction of Celsr1 to particular sides of the cell, but is required for coordinated planar polarization of Celsr1 in node cells (Fig. 6G,H; supplementary material Fig. S3F). We conclude that cofilin activity is required for apical membrane association of PCP proteins, and Wnt ligands are required for their polarized distribution in node cells.

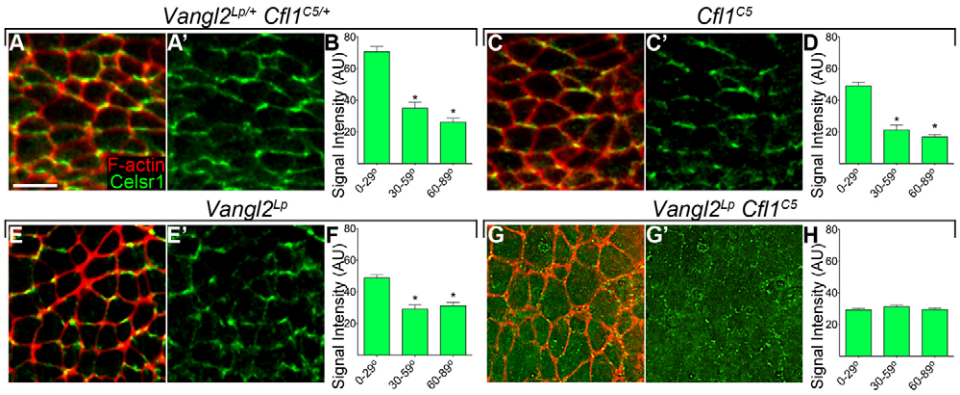

Fig. 5. Celsr1, a core component of the PCP pathway, is not planar polarized in *Vangl2^{Lp} Cfl1^{C5}* double mutants. (**A-B**) Celsr1 (green) is enriched on the anterior/posterior faces of node cells in wild-type embryos. Cell boundaries are highlighted by phalloidin (red), anterior towards the top. (**C-F**) The anterior/posterior enrichment of Celsr1 is retained in *Cfl1^{C5}* mutants (C-D) and *Vangl2^{Lp}* mutants (E-F). (**G-H**) By contrast, Celsr1 is not enriched at the apical membrane in *Vangl2^{Lp} Cfl1^{C5}* double mutants (G-H). (B,D,F,H) The mean intensity of Celsr1 staining normalized to phalloidin intensity along different edges of the cell. Celsr1 intensity was measured along individual cell borders and binned based on the angle with respect to the mediolateral axis of the embryo, such that 0-29° (horizontal) lines correspond to anterior/posterior faces of the cell, and 60-90° (vertical) lines correspond to mediolateral faces of the cell. Scale bar: 10 µm. Data are mean±s.d. *P<0.001.

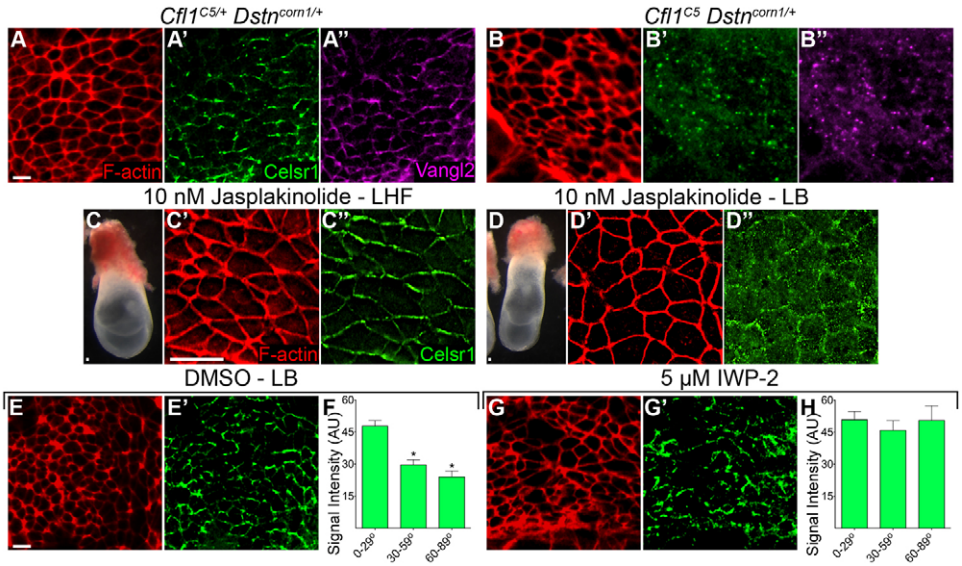

Fig. 6. Decreased cofilin activity is sufficient to disrupt apical trafficking of the PCP proteins Celsr1 and Vangl2. (**A-A″**) The PCP proteins Celsr1 and Vangl2 colocalize to the anterior/posterior faces of node cells in wild-type embryos. (**B-B″**) Celsr1 and Vangl2 colocalize in cytoplasmic puncta in the compound *Cfl1*^{C5} *Dstn*$^{corn1/+}$ mutant. (C-H) Effects of pharmacological inhibitors on the planar polarization of PCP proteins in cultured embryos. (**C-C″**) Late headfold (LHF) stage embryos, shown before culture (C), show normal Celsr1 localization after 14-18 hours of culture in 10 nM jasplakinolide (C″). (**D-D″**) When cultured in the presence of jasplakinolide under the same conditions, earlier embryos (late-bud stage, LB) phenocopy *Vangl2*^{Lp} *Cfl1*^{C5} and *Cfl1*^{C5} *Dstn*$^{corn1/+}$, as Celsr1 fails to become membrane localized (D″). (**E**,**E′**) DMSO control for the late-bud stage culture. (**G**,**G′**) Blocking Wnt ligand secretion does not prevent recruitment of Celsr1 to the membrane, as embryos cultured with 5 µM IWP2 (an inhibitor of Wnt secretion) retain membrane-localized Celsr1, although Celsr1 is present on all faces of node cells. (**F**,**H**) Quantification of the intensity of Celsr1 staining shows normal enrichment to the horizontal (anterior and posterior) edges of node cells in DMSO control (F), which is lost when embryos are cultured with IWP2 (H). Scale bars: 10 µm. Data are mean±s.d. **P*<0.001.

Celsr1 protein was also enriched on the anterior and posterior faces of cells in the notochordal plate of wild-type embryos (Fig. 7A), which require PCP for convergent extension. As in the node, membrane association of Celsr1 was lost when actin remodeling was blocked by culture in the presence of jasplakinolide (Fig. 7B). It has been shown recently that the PCP pathway controls the morphogenetic movements required for neural tube closure in chick embryos by regulating the activation of myosin (Nishimura et al., 2012). Similarly, we found that active phosphorylated myosin light chain 2 (pMLC2) was planar polarized to anterior/posterior faces of cells at the anterior border of the node and the midline (Fig. 7C). This planar polarization of pMLC2 was not detected in the node, where active myosin was distributed uniformly around the circumference of the cells.

Actin severing is required for the coordinated localization of Rab11 and PCP proteins to the plasma membrane

Because disruption of actin severing caused accumulation of Celsr1 and Vangl2 in vesicles in the apical cytoplasm and blocked their localization to the plasma membrane, we hypothesized that actin dynamics might be required to target vesicles that contain these PCP proteins to the apical membrane. We therefore tested whether treatment of embryos with jasplakonolide affected the localization of any specific class of vesicles. We did not detect any change in the distribution of Rab8-, Rab5- or EEA1-associated vesicles in node cells after culture in the presence of jasplakinolide (supplementary material Fig. S7; Fig. 8A-B′). By contrast, Rab11, a marker associated with recycling endosomes, showed an interesting change in distribution in treated embryos. In control embryos, Rab11 was present in both cytoplasmic apical vesicles and in vesicles immediately adjacent to the plasma membrane at the level of the adherens junctions. The membrane-associated Rab11 appeared to be more commonly associated with horizontal faces of cells where Celsr1 was localized (Fig. 8C-C″; supplementary material Fig. S3G), although this association was not statistically significant. Inhibition of actin severing by jasplakinolide treatment caused a clear change in Rab11 distribution: cytoplasmic Rab11^{+} vesicles were still present, but these vesicles were no longer adjacent to the plasma membrane (Fig. 8D-D′; supplementary material Fig. S3H). In addition, ~31% (n=187) of the Celsr1^{+} puncta were also positive for Rab11 in jasplakinolide-treated embryos (Fig. 8D-D″). Although jasplakinolide did not change the localization of the early endosome marker EEA1, 44% (n=157) of the apical Celsr1^{+} puncta were marked by EEA1 in the presence, but not the absence, of jasplakinolide (Fig. 8A-B″). These data suggest that Celsr1 normally moves to the membrane through EEA1 and Rab11-positive vesicles, and that inhibition of actin turnover prevents the fusion of the Rab11^{+} vesicles with the apical plasma membrane.

DISCUSSION

Cofilin and convergent extension of the midline

Our data describe convergent extension of the mouse midline at a cellular level. At the one- to four-somite stage, there are ~200 brachyury (T)-expressing cells in the axial midline anterior to the node, and the cellular arrangement of the T^{+} cells depends on the activity of the PCP pathway. In wild-type and *Cfl1*^{C5} embryos, the midline cells are arranged in a narrow stripe three or four cells wide and ~55 cells long. Confirming previous impressions, the *Vangl2*^{Lp} midline is somewhat wider and shorter (four or five cells wide and ~45 cells long). The *Vangl2*^{Lp} *Cfl1*^{C5} midline is approximately twice

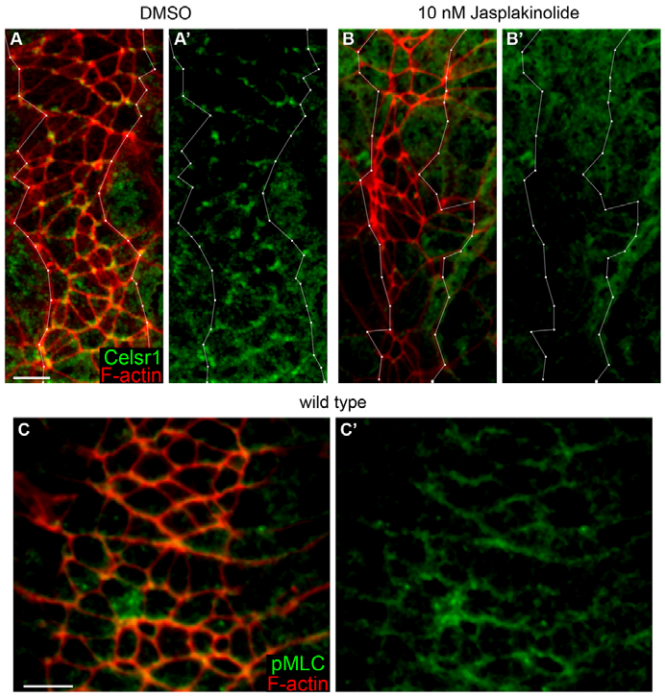

Fig. 7. Celsr1 and phospho-myosin light chain 2 are planar polarized in the axial midline. (**A**,**A′**) In wild-type embryos cultured for 14-18 hours in 0.1% DMSO, Celsr1 (green) is planar polarized to the anterior/posterior faces in the apical membrane of cells in the midline (outlined in white). (**B**,**B′**) Membrane enrichment of Celsr1 is lost when wild-type embryos are cultured in the presence of 10 nM jasplakinolide. (**C**,**C′**) In the midline of wild-type embryos, phospho-myosin light chain 2 (green) is also planar polarized at the apical membrane to the anterior/posterior faces of the cell. Scale bars: 10 μm.

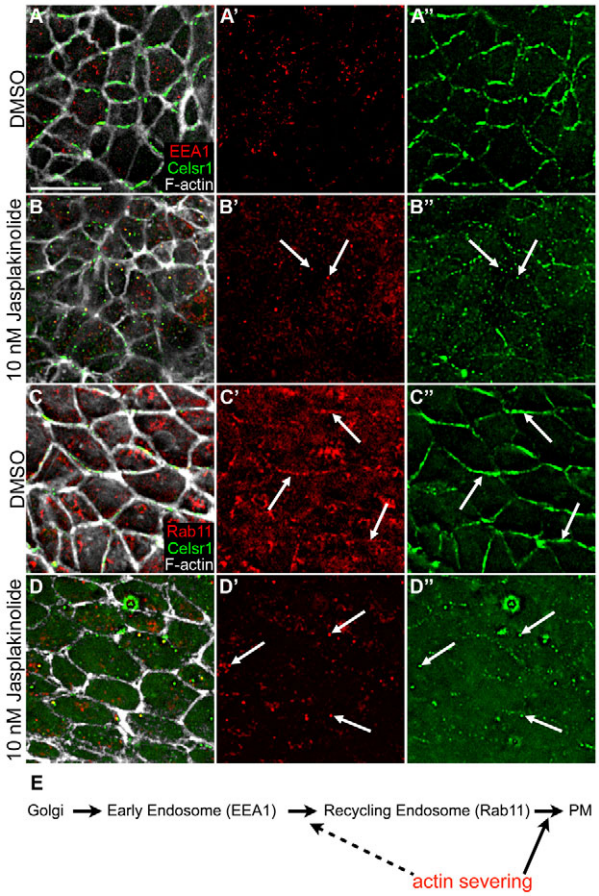

Fig. 8. Treatment with jasplakinolide inhibits plasma membrane association of Rab11 and Celsr1. (**A-A″**) In wild-type embryos cultured for 14 hours in DMSO, there is no colocalization between Celsr1 (green) and the early endosomal marker EEA1 (red). (**B-B″**) Treatment with 10 nM jasplakinolide inhibits plasma membrane association of Celsr1; some cytoplasmic Celsr1 puncta overlaps with EEA1 (arrows). (**C-C″**) In wild-type embryos cultured for 14 hours in DMSO, there is some overlap between Rab11 (red) and Celsr1 adjacent to the plasma membrane (arrows). (**D-D″**) Rab11 colocalizes with some Celsr1 puncta after treatment with jasplakinolide (arrows), although neither Rab11 nor Celsr1 localizes to the plasma membrane. Phalloidin staining (white) marks F-actin. (**E**) Model for trafficking of PCP proteins. Celsr1 and Vangl2 traffic to EEA1$^+$ endosomes then enter Rab11$^+$ vesicles and are delivered to planar polarized complexes at the plasma membrane (PM) at the initiation of PCP in the node. Actin dynamics are required for this last step and possibly for the movement/transition of EEA1$^+$ endosomes to the Rab11 compartment. Scale bar: 10 μm.

as wide and half as long as wild type (six cells wide and ~32 cells long) and significantly shorter and wider than *Vangl2^{Lp}* single mutants. The cells of the midline arise from the node (Hashimoto et al., 2010), and the number of cells across the width of the midline of the double mutants was the same as the number of cells at the anterior edge of the node. Together, this suggests that convergent extension normally leads to a twofold narrowing of the midline in wild type and that this process fails completely in the *Vangl2^{Lp} Cfl1^{C5}* double mutants. After cells exit the node, they intercalate to lengthen and narrow the notochordal plate; our data suggest that this active movement depends on planar polarization of phosphorylated MLC2 at the junction of the node and midline.

Vangl2 and cofilin cooperate to target PCP proteins to the apical membrane

The *Vangl2^{Lp}* mutation provides a sensitized background to identify additional genes required for mammalian PCP. We show that, as in *Vangl1 Vangl2* double-null mutants, planar polarity appears to be abolished in *Vangl2^{Lp} Cfl1^{C5}* double mutants, indicating that Vangl2 and cofilin act in pathways that converge on membrane trafficking of Celsr1. Although defects in membrane trafficking of Celsr1 are not apparent in the *Cfl1^{C5}* single mutants, stronger disruptions of actin severing, caused by either loss-of-function mutations in two cofilin genes or by pharmacological inhibitors of actin severing, blocks membrane localization of PCP proteins. We hypothesize that there are subtle defects in trafficking of PCP vesicles to the membrane in *Cfl1^{C5}* single mutants, and, when combined with Vangl2 deficiency, the trafficking of PCP proteins to the membrane is abolished.

Cofilin and trafficking of Rab11$^+$ vesicles

Our data argue that dynamic rearrangement of F-actin filaments is required to target vesicles containing PCP proteins to the apical plasma membrane. Cofilin has been implicated in several steps of vesicle trafficking. Disruption of cofilin by knockdown or overexpression has been shown to disrupt formation of vesicles from the trans-Golgi network (Salvarezza et al., 2009) or sorting of proteins in the Golgi (von Blume et al., 2009). However, because we observe Celsr1 and Vangl2 in cytoplasmic puncta in a domain apical

to the Golgi in the node cells of *Cfl1*^{C5} *Dstn*$^{corn1/+}$ compound mutants and jasplakinolide-treated embryos, we conclude that a later step in the vesicle trafficking pathway is disrupted in the mutants. Recent genetic experiments in the *C. elegans* intestine indicated that cofilin also regulates the apical distribution of Rab11$^+$ vesicles (Winter et al., 2012). Consistent with those observations, we observe that loss of actin severing disrupts the association of Rab11$^+$ vesicles with the plasma membrane and leads to accumulation of Rab11$^+$ Celsr1$^+$ vesicles in the apical domain of node cells, arguing that Rab11$^+$ vesicles are crucial targets of cofilin-regulated trafficking in PCP. It has previously been shown that planar polarity is maintained through cell division by regulated internalization and retargeting of PCP proteins during mitosis, and more than 70% of the Celsr1$^+$ vesicles are also Rab11$^+$ in that context (Devenport et al., 2011). Our results suggest that the initial targeting of PCP proteins to the cell surface follows a similar pathway. Although Rab11 is important for dynamic relocalization of E-cadherin (Desclozeaux et al., 2008; Classen et al., 2005), E-cadherin localization is not affected in either *Vangl2*^{Lp} *Cfl1*^{C5} double mutants or jasplakinolide-treated embryos, indicating that the PCP proteins are particularly sensitive to disruptions of this trafficking pathway in the node.

The data show that actin stabilization causes a specific defect in the trafficking or docking of Rab11$^+$ vesicles containing PCP proteins to the apical membrane in the node. However, once established within a cell, these PCP complexes are unaffected by actin stabilization. After localization to the apical membrane, interactions among the cytoplasmic PCP proteins and trafficking along the microtubule cytoskeleton are important to maintain PCP proteins on opposite faces of the cell (Shimada et al., 2006). We suggest that the initial targeting of PCP proteins depends on a F-actin-dependent pathway, either through direct targeting of Rab11$^+$ PCP$^+$ vesicles to the plasma membrane or by endocytosis of membrane-associated PCP proteins into a Rab11$^+$ recycling endosome; in either scenario, dynamic reorganization of the apical F-actin cytoskeleton is required for the initial targeting of Rab11$^+$ PCP$^+$ vesicles to the plasma membrane, which ultimately allows planar polarized localization (Fig. 8E).

The activity of cofilin can be regulated by phosphorylation and is downstream of a variety of signals (Bernstein and Bamburg, 2010). The identification of cofilin as a regulator of mammalian planar cell polarity suggests that planar polarity could be modulated through phosphorylation or dephosphorylation of cofilin in response to tissue-specific signals during mammalian development.

Acknowledgements
We thank W. Witke for the *Cfl1*^{tm1Wit} mice, B. Yoder for the *IFT88*$^{tm1.1Bky}$ mice, and F. Conlon, M. Montcouquiol and E. Fuchs for providing antibodies. We thank the MSKCC RARC staff, Nina Lampen at the Electron Microscopy Core Facility and the staff of the Molecular Cytology Core Facility for their expert assistance during SEM and confocal imaging. We thank Jennifer Zallen, Prasad Jallepalli, Michael Overholtzer, Danelle Devenport and members of the Anderson lab for comments on the manuscript, discussions and advice.

Funding
J.G.-B. was supported by a long-term European Molecular Biology Organisation post-doctoral fellowship. The work was supported by National Institutes of Health (NIH) [HD035455 to K.V.A.]. Deposited in PMC for release after 12 months.

Competing interests statement
The authors declare no competing financial interests.

Supplementary material
Supplementary material available online at
http://dev.biologists.org/lookup/suppl/doi:10.1242/dev.085316/-/DC1

References

Axelrod, J. D. (2001). Unipolar membrane association of Dishevelled mediates Frizzled planar cell polarity signaling. *Genes Dev.* **15**, 1182-1187.
Bastock, R., Strutt, H. and Strutt, D. (2003). Strabismus is asymmetrically localised and binds to Prickle and Dishevelled during Drosophila planar polarity patterning. *Development* **130**, 3007-3014.
Bellomo, D., Lander, A., Harragan, I. and Brown, N. A. (1996). Cell proliferation in mammalian gastrulation: the ventral node and notochord are relatively quiescent. *Dev. Dyn.* **205**, 471-485.
Bernstein, B. W. and Bamburg, J. R. (2010). ADF/cofilin: a functional node in cell biology. *Trends Cell Biol.* **20**, 187-195.
Blair, A., Tomlinson, A., Pham, H., Gunsalus, K. C., Goldberg, M. L. and Laski, F. A. (2006). Twinstar, the Drosophila homolog of cofilin/ADF, is required for planar cell polarity patterning. *Development* **133**, 1789-1797.
Bubb, M. R., Senderowicz, A. M., Sausville, E. A., Duncan, K. L. and Korn, E. D. (1994). Jasplakinolide, a cytotoxic natural product, induces actin polymerization and competitively inhibits the binding of phalloidin to F-actin. *J. Biol. Chem.* **269**, 14869-14871.
Chen, B., Dodge, M. E., Tang, W., Lu, J., Ma, Z., Fan, C.-W., Wei, S., Hao, W., Kilgore, J., Williams, N. S. et al. (2009). Small molecule-mediated disruption of Wnt-dependent signaling in tissue regeneration and cancer. *Nat. Chem. Biol.* **5**, 100-107.
Classen, A.-K., Anderson, K. I., Marois, E. and Eaton, S. (2005). Hexagonal packing of Drosophila wing epithelial cells by the planar cell polarity pathway. *Dev. Cell* **9**, 805-817.
Copp, A. J., Greene, N. D. E. and Murdoch, J. N. (2003). Dishevelled: linking convergent extension with neural tube closure. *Trends Neurosci.* **26**, 453-455.
Darken, R. S., Scola, A. M., Rakeman, A. S., Das, G., Mlodzik, M. and Wilson, P. A. (2002). The planar polarity gene strabismus regulates convergent extension movements in Xenopus. *EMBO J.* **21**, 976-985.
Desclozeaux, M., Venturato, J., Wylie, F. G., Kay, J. G., Joseph, S. R., Le, H. T. and Stow, J. L. (2008). Active Rab11 and functional recycling endosome are required for E-cadherin trafficking and lumen formation during epithelial morphogenesis. *Am. J. Physiol.* **295**, C545-C556.
Devenport, D. and Fuchs, E. (2008). Planar polarization in embryonic epidermis orchestrates global asymmetric morphogenesis of hair follicles. *Nat. Cell Biol.* **10**, 1257-1268.
Devenport, D., Oristian, D., Heller, E. and Fuchs, E. (2011). Mitotic internalization of planar cell polarity proteins preserves tissue polarity. *Nat. Cell Biol.* **13**, 893-902.
Eaton, S., Wepf, R. and Simons, K. (1996). Roles for Rac1 and Cdc42 in planar polarization and hair outgrowth in the wing of Drosophila. *J. Cell Biol.* **135**, 1277-1289.
García-García, M. J., Eggenschwiler, J. T., Caspary, T., Alcorn, H. L., Wyler, M. R., Huangfu, D., Rakeman, A. S., Lee, J. D., Feinberg, E. H., Timmer, J. R. et al. (2005). Analysis of mouse embryonic patterning and morphogenesis by forward genetics. *Proc. Natl. Acad. Sci. USA* **102**, 5913-5919.
Greene, N. D., Gerrelli, D., Van Straaten, H. W. and Copp, A. J. (1998). Abnormalities of floor plate, notochord and somite differentiation in the loop-tail (Lp) mouse: a model of severe neural tube defects. *Mech. Dev.* **73**, 59-72.
Gurniak, C. B., Perlas, E. and Witke, W. (2005). The actin depolymerizing factor n-cofilin is essential for neural tube morphogenesis and neural crest cell migration. *Dev. Biol.* **278**, 231-241.
Hashimoto, M., Shinohara, K., Wang, J., Ikeuchi, S., Yoshiba, S., Meno, C., Nonaka, S., Takada, S., Hatta, K., Wynshaw-Boris, A. et al. (2010). Planar polarization of node cells determines the rotational axis of node cilia. *Nat. Cell Biol.* **12**, 170-176.
Jones, C., Roper, V. C., Foucher, I., Qian, D., Banizs, B., Petit, C., Yoder, B. K. and Chen, P. (2008). Ciliary proteins link basal body polarization to planar cell polarity regulation. *Nat. Genet.* **40**, 69-77.
Keller, R. (2002). Shaping the vertebrate body plan by polarized embryonic cell movements. *Science* **298**, 1950-1954.
Koike, S., Keino-Masu, K., Ohto, T., Sugiyama, F., Takahashi, S. and Masu, M. (2009). Autotaxin/lysophospholipase D-mediated lysophosphatidic acid signaling is required to form distinctive large lysosomes in the visceral endoderm cells of the mouse yolk sac. *J. Biol. Chem.* **284**, 33561-33570.
Lee, J. D., Migeotte, I. and Anderson, K. V. (2010). Left-right patterning in the mouse requires Epb4.1l5-dependent morphogenesis of the node and midline. *Dev. Biol.* **346**, 237-246.
Matusek, T., Djiane, A., Jankovics, F., Brunner, D., Mlodzik, M. and Mihály, J. (2006). The Drosophila formin DAAM regulates the tracheal cuticle pattern through organizing the actin cytoskeleton. *Development* **133**, 957-966.
Montcouquiol, M., Sans, N., Huss, D., Kach, J., Dickman, J. D., Forge, A., Rachel, R. A., Copeland, N. G., Jenkins, N. A., Bogani, D. et al. (2006). Asymmetric localization of Vangl2 and Fz3 indicate novel mechanisms for planar cell polarity in mammals. *J. Neurosci.* **26**, 5265-5275.
Nishimura, T., Honda, H. and Takeichi, M. (2012). Planar cell polarity links axes of spatial dynamics in neural-tube closure. *Cell* **149**, 1084-1097.
Nonaka, S., Tanaka, Y., Okada, Y., Takeda, S., Harada, A., Kanai, Y., Kido, M. and Hirokawa, N. (1998). Randomization of left-right asymmetry due to loss

of nodal cilia generating leftward flow of extraembryonic fluid in mice lacking KIF3B motor protein. *Cell* **95**, 829-837.
Nonaka, S., Shiratori, H., Saijoh, Y. and Hamada, H. (2002). Determination of left-right patterning of the mouse embryo by artificial nodal flow. *Nature* **418**, 96-99.
Nonaka, S., Yoshiba, S., Watanabe, D., Ikeuchi, S., Goto, T., Marshall, W. F. and Hamada, H. (2005). De novo formation of left-right asymmetry by posterior tilt of nodal cilia. *PLoS Biol.* **3**, e268.
Park, M. and Moon, R. T. (2002). The planar cell-polarity gene stbm regulates cell behaviour and cell fate in vertebrate embryos. *Nat. Cell Biol.* **4**, 20-25.
Ross, A. J., May-Simera, H., Eichers, E. R., Kai, M., Hill, J., Jagger, D. J., Leitch, C. C., Chapple, J. P., Munro, P. M., Fisher, S. et al. (2005). Disruption of Bardet-Biedl syndrome ciliary proteins perturbs planar cell polarity in vertebrates. *Nat. Genet.* **37**, 1135-1140.
Salvarezza, S. B., Deborde, S., Schreiner, R., Campagne, F., Kessels, M. M., Qualmann, B., Caceres, A., Kreitzer, G. and Rodriguez-Boulan, E. (2009). LIM kinase 1 and cofilin regulate actin filament population required for dynamin-dependent apical carrier fission from the trans-Golgi network. *Mol. Biol. Cell* **20**, 438-451.
Shimada, Y., Yonemura, S., Ohkura, H., Strutt, D. and Uemura, T. (2006). Polarized transport of Frizzled along the planar microtubule arrays in Drosophila wing epithelium. *Dev. Cell* **10**, 209-222.
Shinohara, K., Kawasumi, A., Takamatsu, A., Yoshiba, S., Botilde, Y., Motoyama, N., Reith, W., Durand, B., Shiratori, H. and Hamada, H. (2012). Two rotating cilia in the node cavity are sufficient to break left-right symmetry in the mouse embryo. *Nat. Commun.* **3**, 622.
Smith, R. S., Hawes, N. L., Kuhlmann, S. D., Heckenlively, J. R., Chang, B., Roderick, T. H. and Sundberg, J. P. (1996). Corn1: a mouse model for corneal surface disease and neovascularization. *Invest. Ophthalmol. Vis. Sci.* **37**, 397-404.
Song, H., Hu, J., Chen, W., Elliott, G., Andre, P., Gao, B. and Yang, Y. (2010). Planar cell polarity breaks bilateral symmetry by controlling ciliary positioning. *Nature* **466**, 378-382.
Strutt, D. I. (2001). Asymmetric localization of frizzled and the establishment of cell polarity in the Drosophila wing. *Mol. Cell* **7**, 367-375.
Strutt, H. and Strutt, D. (2008). Differential stability of flamingo protein complexes underlies the establishment of planar polarity. *Curr. Biol.* **18**, 1555-1564.
Strutt, D. I., Weber, U. and Mlodzik, M. (1997). The role of RhoA in tissue polarity and Frizzled signalling. *Nature* **387**, 292-295.
Sulik, K., Dehart, D. B., Iangaki, T., Carson, J. L., Vrablic, T., Gesteland, K. and Schoenwolf, G. C. (1994). Morphogenesis of the murine node and notochordal plate. *Dev. Dyn.* **201**, 260-278.
Tree, D. R. P., Shulman, J. M., Rousset, R., Scott, M. P., Gubb, D. and Axelrod, J. D. (2002). Prickle mediates feedback amplification to generate asymmetric planar cell polarity signaling. *Cell* **109**, 371-381.
Usui, T., Shima, Y., Shimada, Y., Hirano, S., Burgess, R. W., Schwarz, T. L., Takeichi, M. and Uemura, T. (1999). Flamingo, a seven-pass transmembrane cadherin, regulates planar cell polarity under the control of Frizzled. *Cell* **98**, 585-595.
Veeman, M. T., Slusarski, D. C., Kaykas, A., Louie, S. H. and Moon, R. T. (2003). Zebrafish prickle, a modulator of noncanonical Wnt/Fz signaling, regulates gastrulation movements. *Curr. Biol.* **13**, 680-685.
Vinson, C. R. and Adler, P. N. (1987). Directional non-cell autonomy and the transmission of polarity information by the frizzled gene of Drosophila. *Nature* **329**, 549-551.
von Blume, J., Duran, J. M., Forlanelli, E., Alleaume, A.-M., Egorov, M., Polishchuk, R., Molina, H. and Malhotra, V. (2009). Actin remodeling by ADF/cofilin is required for cargo sorting at the trans-Golgi network. *J. Cell Biol.* **187**, 1055-1069.
Wallingford, J. B. and Harland, R. M. (2002). Neural tube closure requires Dishevelled-dependent convergent extension of the midline. *Development* **129**, 5815-5825.
Wang, J., Hamblet, N. S., Mark, S., Dickinson, M. E., Brinkman, B. C., Segil, N., Fraser, S. E., Chen, P., Wallingford, J. B. and Wynshaw-Boris, A. (2006). Dishevelled genes mediate a conserved mammalian PCP pathway to regulate convergent extension during neurulation. *Development* **133**, 1767-1778.
Winter, C. G., Wang, B., Ballew, A., Royou, A., Karess, R., Axelrod, J. D. and Luo, L. (2001). Drosophila Rho-associated kinase (Drok) links Frizzled-mediated planar cell polarity signaling to the actin cytoskeleton. *Cell* **105**, 81-91.
Winter, J. F., Höpfner, S., Korn, K., Farnung, B. O., Bradshaw, C. R., Marsico, G., Volkmer, M., Habermann, B. and Zerial, M. (2012). Caenorhabditis elegans screen reveals role of PAR-5 in RAB-11-recycling endosome positioning and apicobasal cell polarity. *Nat. Cell Biol.* **14**, 666-676.
Wu, J. and Mlodzik, M. (2008). The frizzled extracellular domain is a ligand for Van Gogh/Stbm during nonautonomous planar cell polarity signaling. *Dev. Cell* **15**, 462-469.
Ybot-Gonzalez, P., Savery, D., Gerrelli, D., Signore, M., Mitchell, C. E., Faux, C. H., Greene, N. D. E. and Copp, A. J. (2007). Convergent extension, planar-cell-polarity signalling and initiation of mouse neural tube closure. *Development* **134**, 789-799.